Coexistence of a self-induced transparency soliton and a Bragg soliton

Hong-Yih Tseng* and Sien Chi
Institute of Electro-Optical Engineering, National Chiao-Tung University, 1001 Ta Hsueh Road, Hsinchu, Taiwan 300, Republic of China
(Received 13 November 2001; published 20 November 2002)

We theoretically show that a self-induced transparency (SIT) soliton and a Bragg soliton can coexist in a nonlinear photonic band gap (PBG) medium doped uniformly with inhomogeneous-broadening two-level atoms. The Maxwell-Bloch equations for the pulse propagating through such a uniformly doped PBG structure are derived first and further reduced to an effective nonlinear Schrödinger equation. This model describes an equivalent physical mechanism for a Bragg-soliton propagation resulting from the effective quadratic dispersion balancing with the effective third-order nonlinearity. Because the resonant atoms are taken into account, the original band gap can be shifted both by the dopants and the instantaneous nonlinearity response originating from an intense optical pulse. As a result, even if a SIT soliton with its central frequency deep inside the original forbidden band, it still can propagate through the resonant PBG medium as long as this SIT soliton satisfies the effective Bragg-soliton propagation. An approximate soliton solution describing such coexistence is found. We also show that the pulse width and group velocity of this soliton solution can be uniquely determined for given material parameters, atomic transition frequency, and input central frequency of the soliton. The numerical examples of the SIT soliton in a one-dimensional As_2S_3-based PBG structure doped uniformly with Lorentzian line-shape resonant atoms are shown. It is found that a SIT soliton with ~100-ps width in such a resonant PBG structure can travel with the velocity being two orders of magnitude slower than the light speed in an unprocessed host medium.

DOI: 10.1103/PhysRevE.66.056606 PACS number(s): 42.65.Tg, 42.70.Qs, 42.50.Md

I. INTRODUCTION

The photonic band gap material has been widely investigated since Yablonovitch [1] and John [2] introduced that a periodic dielectric structure (photonic crystal) exhibits a forbidden band for optical energy. Such a photonic band gap (PBG) results from the coherent multiple scattering of light in the periodic structure. The simplest PBG structure is the fiber Bragg grating, which has been widely applied in the practical light wave communication systems. Although a PBG material has a photonic band gap, the material nonlinearity can render the PBG ''transparent'' for nonlinear optical propagation [3–15]. For example, gap solitons refer to solitary localization and solitary propagation of optical waves in a nonlinear PBG structure [3–10]. The central frequency of a gap soliton is deep inside the forbidden band. The experimental observation of gap solitons in a fiber Bragg grating [9] or in an integrated AlGaAs waveguide grating [10] has been reported. Moreover, a nonlinear PBG medium also can support solitons of an effective nonlinear Schrödinger (NLS) equation [11]. Such a soliton is called a Bragg soliton and its central frequency is close to the band gap edge [12–15]. Bragg solitons have also been successfully observed in fiber Bragg gratings [12]. The experimental results agree well with the NLS model [13–15].

Another example of nonlinear optical pulse propagating through a band gap material is the self-induced transparency (SIT) soliton in a resonant PBG medium [16–23]. SIT solitons are coherent optical pulses propagating through a resonant medium without loss and distortion. Such coherent propagation is described by the Maxwell-Bloch equations [24–30]. For the SIT in a uniformly doped nonlinear PBG structure, Aközbek and John have reported the fundamental work on soliton solutions for frequency detuned near the PBG edge, and call them SIT-gap solitons [22]. Because the dopant density and the atomic detuning frequency dramatically change the characteristics of a SIT-gap soliton, it has been suggested that such solitary propagation may be very useful in optical telecommunications and optical computing. Recently, we have shown that a moving SIT pulse train can exist in a uniformly doped PBG structure [23]. However, the single SIT soliton with its central frequency being deep inside the forbidden gap has not yet been found.

In this paper, we show that a soliton can exist in a uniformly doped nonlinear PBG medium, even if its central frequency is deep inside the stop band. This soliton solution indicates the coexistence of a SIT soliton and a Bragg soliton. The physical mechanism for this coexistence is attributed to the fact that a uniformly doped PBG structure can be regarded as an effective undoped PBG structure. Because the resonant atoms dominate the effective quadratic dispersion and the effective third-order nonlinearity, the original forbidden band has been shifted by the dopants. Furthermore, an instantaneous nonlinearity response due to the intense pulse also shifts the original stop band. As a result, the SIT effect renders the uniformly doped nonlinear PBG ''transparent'' and an optical pulse satisfying the effective Bragg soliton propagation can propagate through this PBG structure. The derivation for this soliton solution is explicitly presented. The numerical examples of such a soliton in an As_2S_3-based PBG structure doped uniformly with Lorentzian line-shape two-level atoms are also shown.

This paper is structured as follows: In Sec. II, the Maxwell-Bloch equations governing the optical pulse propagating in a uniformly doped PBG structure are derived. In

*FAX: 886-3-571-6631. Email address: dabin.eo86g@nctu.edu.tw

 ©2002 The American Physical Society

Sec. III, we reduce the Maxwell-Bloch equations to an effective NLS equation and obtain its soliton solution. This solution is the SIT-Bragg soliton propagating in a resonant PBG structure. In Sec. IV, we study the characteristics of the soliton solution by assuming the inhomogeneous-broadening line shape of the resonant atoms to be Lorentzian. The reduction of the soliton's velocity by both the SIT effect and multiple Bragg scattering in such a resonant PBG medium is also studied. In Sec. V, we compare our results with the previous ones and conclude this paper.

II. MAXWELL-BLOCH EQUATIONS

In this paper, we adopt a one-dimensional Bragg grating formed in a host medium with Kerr nonlinearity as our PBG model. The two-level atoms are uniformly embedded in this Kerr host medium. From Maxwell's equations, the wave equation describing the light propagation in such a medium can be written as

$$\nabla^2\mathbf{E}-\frac{1}{c^2}\frac{\partial^2\mathbf{E}}{\partial t^2}-\mu_0\frac{\partial^2\mathbf{P}}{\partial t^2}=\mu_0\frac{\partial^2\mathbf{P}_R}{\partial t^2}, \tag{2.1}$$

where $\mathbf{E}$ is the electric field in the medium, $\mathbf{P}$ is the electric-induced polarization including the linear and nonlinear contributions of the host medium, $\mathbf{P}_R$ is the resonant polarization resulting from the two-level atoms, c is the velocity of light in vacuum, and μ_0 is the vacuum permeability. The electric field $\mathbf{E}$ propagating along the z direction in such a uniformly doped PBG structure can be expressed as

$$\mathbf{E}(\mathbf{r},t)=\frac{1}{2}\hat{x}F(x,y)\{[E_+(z,t)e^{i(\beta_g z-\omega_B t)} + E_-(z,t)e^{i(-\beta_g z-\omega_B t)}]+\text{c.c.}\}, \tag{2.2}$$

where E_+ and E_- are the envelopes of the forward and Bragg scattering fields, $F(x,y)$ is the transverse modal distribution, $\omega_B=2\pi c/\lambda_B$ is the Bragg frequency, and λ_B is the Bragg wavelength. Moreover, the macroscopic resonant polarization $\mathbf{P}_R$ caused by the dopants is written as

$$\mathbf{P}_R(\mathbf{r},t)=\frac{1}{2}\hat{x}F(x,y)\{[P_+(z,t)e^{i(\beta_g z-\omega_B t)} + P_-(z,t)e^{i(-\beta_g z-\omega_B t)}]+\text{c.c.}\}, \tag{2.3}$$

where P_+ and P_- correspond to the polarization envelopes induced by E_+ and E_-, respectively. In Fourier domain, Eq. (2.1) becomes

$$\nabla^2\tilde{\mathbf{E}}+\tilde{n}(\omega)^2\frac{\omega^2}{c^2}\tilde{\mathbf{E}}=-\mu_0\omega^2\tilde{\mathbf{P}}_R, \tag{2.4}$$

where $\tilde{\mathbf{E}}$ is the Fourier transform of $\mathbf{E}$, $\tilde{\mathbf{P}}_R$ is the Fourier transform of $\mathbf{P}_R$, and $\tilde{n}(\omega)=n(\omega)+n_2|\mathbf{E}|^2+\delta n_g\cos(2\beta_g z)$ is the refractive index of the periodic structure. Here $n(\omega)$ represents the frequency-dependent refractive index of the host medium, n_2 is the Kerr nonlinear-index coefficient, δn_g is the magnitude of the periodic-index variation, $\beta_g=\pi/\Lambda_g$ is the grating wave number, Λ_g is the grating period which satisfies the Bragg condition $\Lambda_g=\lambda_B/(2\bar{n})$, and $\bar{n}$ is the average refractive index of the medium.

To obtain the pulse propagation equations for this uniformly doped PBG structure, we use the perturbation theory of distributed feedback [31] to reduce Eq. (2.4). The dielectric constant $\tilde{n}(\omega)^2$ in Eq. (2.4) is approximated by

$$\tilde{n}(\omega)^2\approx n(\omega)^2+2n(\omega)[n_2|\mathbf{E}|^2+\delta n_g\cos(2\beta_g z)]. \tag{2.5}$$

Substituting Eqs. (2.2), (2.3), and (2.5) into Eq. (2.4) yields the following equations:

$$\frac{\partial^2F}{\partial x^2}+\frac{\partial^2F}{\partial y^2}+[k_0^2n(\omega)^2-\tilde{\beta}_\pm(\omega)^2]F=0, \tag{2.6a}$$

$$\frac{\partial^2\tilde{E}_\pm}{\partial z^2}\pm 2j\beta_g\frac{\partial\tilde{E}_\pm}{\partial z}+[\tilde{\beta}_\pm(\omega)^2-\beta_g^2]\tilde{E}_\pm+2k_0^2n(\omega)\delta n_g\tilde{E}_\mp = -u_0\omega^2\tilde{P}_\pm, \tag{2.6b}$$

where $k_0=\omega/c$, $\tilde{\beta}_\pm(\omega)$ are the wave numbers that are determined according to the eigenvalues of Eq. (2.6a), $\tilde{E}_\pm$ is the Fourier transform of $E_\pm$, and $\tilde{P}_\pm$ is the Fourier transform of $P_\pm$. The transverse mode function $F(x,y)$ can be averaged out by introducing the effective core area A_{eff} [31]. Likewise the averaged effects of the coupling strength and the Kerr nonlinearity can be described by

$$\kappa=\frac{k_0\int_{-\infty}^{\infty}\int_{-\infty}^{\infty}\delta n_g|F(x,y)|^2dx\,dy}{\int_{-\infty}^{\infty}\int_{-\infty}^{\infty}|F(x,y)|^2dx\,dy}$$

and

$$\Delta\beta_\pm=\frac{k_0\int_{-\infty}^{\infty}\int_{-\infty}^{\infty}\Delta n_\pm|F(x,y)|^2dx\,dy}{\int_{-\infty}^{\infty}\int_{-\infty}^{\infty}|F(x,y)|^2dx\,dy}, \tag{2.7}$$

respectively. Here $\Delta n_\pm\equiv n_2(|\tilde{E}_\pm|^2+2|\tilde{E}_\mp|^2)$ indicate the nonlinear effects of self-phase modulation and cross-phase modulation. In the perturbation theory, $\Delta n_\pm$ do not affect the modal distribution $F(x,y)$. However, the eigenvalues $\tilde{\beta}_\pm(\omega)$ are given by $\tilde{\beta}_\pm(\omega)=\beta(\omega)+\Delta\beta_\pm$, where $\beta(\omega)=(\omega/c)n(\omega)$ is the mode-propagation constant of the electric field. Under the slowly varying envelope approximation, Eq. (2.6b) can be reduced to

$$\pm j\frac{\partial\tilde{E}_\pm}{\partial z}+[\beta(\omega)-\beta_g]\tilde{E}_\pm+\Delta\beta_\pm\tilde{E}_\pm+\kappa\tilde{E}_\mp = -\frac{\mu_0}{2\beta_g}\omega^2\tilde{P}_\pm. \tag{2.8}$$

In obtaining Eq. (2.8), we have used $\tilde{\beta}(\omega)^2-\beta_g^2 \approx 2\beta_g[\tilde{\beta}(\omega)-\beta_g]$ and $\beta(\omega)/\beta_g \approx 1$, which indicate that the grating wave number is close to the mode-propagation constant. Taking the inverse Fourier transform of Eq. (2.8) results in the time-domain propagation equations. For this purpose, we regard $\Delta\beta_\pm$ as constant perturbation and expand both ω^2 and $\beta(\omega)$ in Taylor series near the Bragg frequency ω_B, i.e., $\omega^2 \approx \omega_B^2 + 2\omega_B(\omega-\omega_B)$ and $\beta(\omega) \approx \beta_0 + (\omega-\omega_B)\beta_1$, where $\beta_j = d^j\beta/d\omega^j|_{\omega-\omega_B}$ $(j=0,1)$, and the second-order and higher-order terms in the expansion have been neglected. Consequently, the time-domain coupled-mode equations that describe pulse propagating in a uniformly doped PBG structure can be written as

$$\pm i\frac{\partial E_\pm}{\partial z} + i\beta_1\frac{\partial E_\pm}{\partial t} + \delta\beta_0 E_\pm + \kappa E_\mp + \Gamma(|E_\pm|^2 + 2|E_\mp|^2)E_\pm + \frac{\mu_0\omega_B^2}{2\beta_g}\left(P_\pm + \frac{2i}{\omega_B}\frac{\partial P_\pm}{\partial t}\right) = 0, \tag{2.9}$$

where $\delta\beta_0 = \beta_0 - \beta_g$ implies the wave number detuning from the exact Bragg resonance, and $\Gamma = n_2\omega_B/(cA_{\text{eff}})$ is the Kerr nonlinearity coefficient. Note that all the second derivatives of $E_\pm$ and $P_\pm$ with respect to z and t have been neglected by using the slowly varying envelope approximation.

The coherent interactions between the electric field and the two-level atoms can be described by the atomic Bloch equations. To express the Bloch equations, we first assume the complex envelopes $E_\pm$ and $P_\pm$ can be further written as

$$E_\pm(z,t) = a_\pm(z,t)\exp[i\varphi_\pm(z,t)], \tag{2.10a}$$

$$P_\pm(z,t) = [U_\pm(z,t) + iV_\pm(z,t)]\exp[i\varphi_\pm(z,t)], \tag{2.10b}$$

where $a_\pm$ are real envelopes, $\varphi_\pm$ are phase functions, $U_\pm$ correspond to the dispersion induced by the resonant atoms, and $V_\pm$ correspond to the absorption caused by the resonant atoms. Moreover, the Bloch vectors $(u_\pm, \nu_\pm, w)$ relate the macroscopic polarization and population difference as follows:

$$(U_\pm, V_\pm, W) = \int_{-\infty}^{\infty}(u_\pm, \nu_\pm, w)g(\Delta\omega-\Delta\omega_{r0})d(\Delta\omega), \tag{2.11}$$

where $\Delta\omega$ is defined by $\Delta\omega = \omega_r - \omega_B$, $(u_\pm, \nu_\pm, w)$ describe the components of the polarization and population difference contributed from the atoms with resonant frequencies in the whole range of $\Delta\omega$, $g(\Delta\omega-\Delta\omega_{r0})$ is the normalized inhomogeneous-broadening line-shape function, $\Delta\omega_{r0}$ is defined by $\Delta\omega_{r0} = \omega_{r0} - \omega_B$, and ω_{r0} is the center of the broadening line-shape function. Here, the quantity $W = \mu(N_1 - N_2)$ is the macroscopic population difference multiplied by the transition matrix element μ between the ground state (N_1) and the upper state (N_2) of the two-level system. Furthermore, to keep a closed set of the Bloch equations, we assume $\varphi_\pm(z,t) = \phi(z,t) \pm \psi(z,t)$ and $w = w_0 + 2w_1\cos[2\psi(z,t) + 2\beta_g z]$. After neglecting the atomic relaxation times and the terms oscillating as $\exp(\pm i3\beta_g z)$, we can express the atomic Bloch equations as [23]

$$\frac{\partial u_\pm}{\partial t} = \left(\Delta\omega + \frac{\partial\varphi_\pm}{\partial t}\right)\nu_\pm, \tag{2.12a}$$

$$\frac{\partial \nu_\pm}{\partial t} = -\left(\Delta\omega + \frac{\partial\varphi_\pm}{\partial t}\right)u_\pm + \frac{\mu}{\hbar}(a_\pm w_0 + a_\mp w_1), \tag{2.12b}$$

$$\frac{\partial w_0}{\partial t} = \frac{\mu}{\hbar}(a_+\nu_+ + a_-\nu_-), \tag{2.12c}$$

$$\frac{\partial w_1}{\partial t} = -\frac{\mu}{2\hbar}(a_+\nu_- + a_-\nu_+). \tag{2.12d}$$

The neglecting of the terms oscillating as $\exp(\pm i3\beta_g z)$ indicates that this paper is devoted to finding a single-pulse solution propagating along one direction (like a Bragg soliton), and exciting no higher-order spatial harmonic of population difference [22,23].

III. APPROXIMATE SOLITON SOLUTION TO THE MAXWELL-BLOCH EQUATIONS

In this section, we reduce the Maxwell-Bloch equations to the effective NLS equation for the optical pulse propagating in a nonlinear PBG structure doped uniformly with inhomogeneous-broadening two-level atoms. The atomic Bloch equations can be solved by using the factorization ansatz $\nu_\pm(\Delta\omega,z,t) = \nu_1^\pm(0,z,t)f(\Delta\omega)$, where $f(\Delta\omega) = (1 + c_1\Delta\omega + c_2\Delta\omega^2)^{-1}$ is the dipole spectra-response function of the resonant atoms [22,23,25,27,29]. Because such an ansatz can lead to a self-consistent solution to the Maxwell-Bloch equations, it has been widely applied to solve the SIT problems. The undetermined constants c_1 and c_2 both relate to the frequency detuning and the pulse width of the electric field, and they will be identified in the following section. Using the factorization ansatz [23], we have

$$u_\pm = \left[c_1 - \left(\frac{\partial\varphi_\pm}{\partial t} - \Delta\omega\right)c_2\right]\frac{\mu}{\hbar}w_i f(\Delta\omega)a_\pm(z,t), \tag{3.1a}$$

$$\nu_\pm = c_2\frac{\mu}{\hbar}w_i f(\Delta\omega)\frac{\partial}{\partial t}a_\pm(z,t), \tag{3.1b}$$

$$w_0 = w_i - \frac{c_2}{2}\left(\frac{\mu}{\hbar}\right)^2 w_i f(\Delta\omega)[a_+^2(z,t) + a_-^2(z,t)], \tag{3.1c}$$

$$w_1 = -\frac{c_2}{2}\left(\frac{\mu}{\hbar}\right)^2 w_i f(\Delta\omega)[a_+(z,t)a_-(z,t)], \tag{3.1d}$$

where $w_i = N_D\mu$ is the initial population difference, and $N_D = N_1 + N_2$ is the doping concentration of the resonant at-

oms. The initial population difference is in the ground state of the two-level system. Substituting Eqs. (3.1) into Eqs. (2.12a) and (2.12b), we have

$$2\frac{\partial a_{\pm}}{\partial t}\frac{\partial \varphi_{\pm}}{\partial t}+\frac{\partial^2 \varphi_{\pm}}{\partial t^2}a_{\pm}=\frac{c_1}{c_2}\frac{\partial a_{\pm}}{\partial t}, \tag{3.2a}$$

$$\frac{\partial^2 a_{\pm}}{\partial t^2}=\left[\frac{1}{c_2}-\frac{c_1}{c_2}\left(\frac{\partial \varphi_{\pm}}{\partial t}\right)+\left(\frac{\partial \varphi_{\pm}}{\partial t}\right)^2\right]a_{\pm} - \frac{\mu^2}{2\hbar^2}(a_{\pm}^2+2a_{\mp}^2)a_{\pm}. \tag{3.2b}$$

Now we define $s=\mu_0\omega_B^2 w_i\mu/(2\beta_g\hbar)$ and two integral constants

$$I_1=\int_{-\infty}^{\infty} f(\Delta\omega)g(\Delta\omega-\Delta\omega_{r0})d(\Delta\omega), \tag{3.3a}$$

$$I_2=\int_{-\infty}^{\infty} \Delta\omega f(\Delta\omega)g(\Delta\omega-\Delta\omega_{r0})d(\Delta\omega). \tag{3.3b}$$

Then substituting Eqs. (2.10), (2.11), and (3.1)–(3.3) into Eqs. (2.9), we obtain

$$\pm i\frac{\partial E_{\pm}}{\partial z}+i\beta_1^e\frac{\partial E_{\pm}}{\partial t}+\delta\beta_e E_{\pm}+\kappa E_{\mp}+\Gamma_e(|E_{\pm}|^2 +2|E_{\mp}|^2)E_{\pm}=0, \tag{3.4}$$

where the effective parameters are

$$\delta\beta_e=\delta\beta_0+sc_1I_1-(2sI_1/\omega_B)+sc_2I_2, \tag{3.5a}$$

$$\beta_1^e=\beta_1+sc_2I_1+2sc_2I_2/\omega_B, \tag{3.5b}$$

$$\Gamma_e=\Gamma+sc_2I_1\mu^2/(\omega_B\hbar^2). \tag{3.5c}$$

Therefore, Eq. (2.9) is reduced to effective nonlinear coupled-mode equations (NLCMEs) under the slowly varying envelope approximation. The effective NLCMEs describe that a uniformly doped PBG structure can be modeled by an effective PBG structure without dopants. Consequently, many of the results known for the NLCMEs can be easily applied to clarify the existence of the SIT soliton in a nonlinear doped PBG structure. We stress that the analytic solutions describing the pulse propagation in a doped nonlinear PBG structure have to satisfy both Eqs. (3.2) and (3.4). We call Eqs. (3.2) and (3.4) the Bloch-NLCMEs.

The NLCMEs in the form of Eq. (3.4) have exact gap-soliton solutions [3–8]; however, such an exact single-pulse solution cannot satisfy Eqs. (3.2). The exact solution to both Eqs. (3.2) and (3.4) is a distortionless pulse-train solution given by sinusoidal functions with a dc background and a modulated phase [23]. In this paper, we try to find out a single-pulse solitary wave in a uniformly doped nonlinear PBG structure. Hence we focus our study on an approximate solution such as a Bragg soliton in an undoped fiber grating. The linear terms of Eq. (3.4) are considered first. Their dispersion relation is written as $\Omega=\omega-\omega_B'=\pm\sqrt{Q^2+\kappa^2}/\beta_1^e \equiv \Omega_{\pm}$, where Ω and Q are the frequency and wave number detuning from the effective Bragg resonance ω_B'. According to Eq. (3.5a), the equivalent Bragg frequency has been shifted to $\omega_B'=\omega_B-(-\delta\beta_e/\beta_1^e)$ because of the resonant atoms. It is known that the original Bragg wavelength is $\lambda_B=2\bar{n}\Lambda_g$. The lower Bragg frequency ω_B' points out that the effective index in a uniformly doped PBG structure is greater than that in a pure PBG structure. Accordingly, the effective velocity $1/\beta_1^e$, indicated by Eq. (3.5b), is slower than that in a pure material. Here we define $\Delta\omega_B=-\delta\beta_e/\beta_1^e$ and $\Delta\omega_0=\omega_0-\omega_B$, where ω_0 is the input carrier frequency of the electric field. Figure 1 schematically shows the frequency detuning $\Delta\omega_0$ with repect to the dispersion relations. The hyperbolic curves $\Omega_{\pm}^0$ indicate the original dispersion relation of the PBG structure without dopants, and $\Omega_{\pm}$ indicate the effective dispersion relation associated with the linear terms of Eq. (3.4), i.e., $\Omega_{\pm}^0$ are identical to $\Omega_{\pm}|_{N_D=0}$. The center of the original gap is located at ω_B, and this original gap has a width equal to $2\kappa/\beta_1$. After we take into account the effects from the resonant atoms, not only the Bragg frequency is shifted to ω_B', but also the width of this effective gap is narrowed to $2\kappa/\beta_1^e$ because of the larger effective index. The Bloch waves (linear eigenstates) corresponding to $\Omega_{\pm}$ are exact solutions to the linear terms of Eq. (3.4). In addition, the group velocity of the Bloch wave on the upper branch is $\nu_g=\partial\Omega_+/\partial Q$; thus we have $\Omega_+=\kappa\gamma/\beta_1^e$ and $Q=\nu\kappa\gamma$ by defining $\nu=\beta_1^e\nu_g$ and $\gamma=1/\sqrt{1-\nu^2}$. The solution to Eq. (3.4) now can be treated as the envelope function of the Bloch wave corresponding to the upper band gap edge [4–5,11–15,31]. Such an envelope function expressed as $\mathsf{E}(z,t)$ describes how the positive nonlinearity weakly modulates the Bloch wave. Consequently, under the limitations of low intensity, the effective NLCMEs for

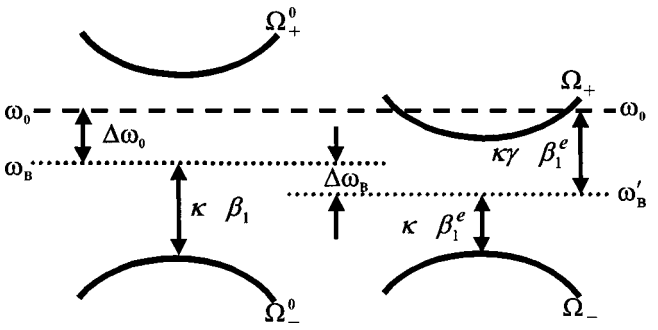

FIG. 1. Frequency detuning of $E_{\pm}$ with respect to the original dispersion relation $\Omega_{\pm}^0$ of the PBG structure, and the effective dispersion relation $\Omega_{\pm}$ for the linear terms of Eq. (3.4).

$$E_{\pm}(\xi,\tau)\approx\pm\left(\frac{1\pm\nu}{2}\right)^{1/2}\mathsf{E}(\xi,\tau)e^{i(Qz-\Omega_+ t)}e^{-i(-\Delta\omega_B t)} \tag{3.6}$$

can be well approximated by an effective NLS equation [14,31]

$$i\frac{\partial \mathsf{E}}{\partial\xi}-\frac{1}{2}\beta_2^e\frac{\partial^2\mathsf{E}}{\partial\tau^2}+\Gamma_\nu|\mathsf{E}|^2\mathsf{E}=0, \tag{3.7}$$

where $\tau=t-z/v_g$ and $\xi=z$ are the moving frame coordinates, and the parameters of this NLS equation depend on the effective undoped PBG structure via

$$\Gamma_\nu=\frac{3-\nu^2}{2\nu}\Gamma_e, \quad \beta_2^e=-(\beta_1^e)^2\frac{1}{\kappa\gamma^3\nu^3}. \tag{3.8}$$

Although Eq. (3.7) has well-known Bragg-soliton solutions, the solution to Eq. (3.7) has to satisfy Eqs. (3.2) obtained from the Bloch equations. Notice that the reduction from Eq. (3.4) to Eq. (3.7) is valid at any soliton velocity [15]. However, to satisfy Eqs. (3.2), we use the slow-velocity ($\nu\ll 1$) limit [5] so that $E_\pm(\xi,\tau)$ are written as $E_\pm(\xi,\tau)\approx \pm\mathsf{E}(\xi,\tau)\exp[i(Qz-\Omega_+ t)+i\Delta\omega_B t]/\sqrt{2}$ approximately. In addition, we seek the solution in the form of

$$\mathsf{E}(\xi,\tau)=a(\tau)\exp[i\varphi(\tau)+i\xi/(2L_D)], \tag{3.9}$$

where L_D is the dispersion length representing the length scale over which the dispersive effects are important. Integrating Eq. (3.2a) and using $a_\pm(z,t)=\pm\mathsf{E}(\xi,\tau)|/\sqrt{2}=\pm a(\tau)/\sqrt{2}$, we obtain

$$\frac{\partial\varphi_+}{\partial\tau}=\frac{\partial\varphi_-}{\partial\tau}=\frac{c_1}{2c_2}+\frac{2c_0}{a(\tau)^2}, \tag{3.10}$$

where c_0 is an integration constant, and we set $\Delta\omega_0=-\Delta\omega_B+\Omega_+=-c_1/(2c_2)$ and $\partial\varphi/\partial\tau=2c_0/a(\tau)^2$. Equation (3.10) describes the general phase modulation, or pulse chirping in the SIT. The constant $-c_1/(2c_2)$ indicates that the carrier frequency of the optical field is $\omega_B-c_1/(2c_2)$; moreover, the instantaneous frequency is inversely proportional to the pulse intensity. Such a chirping relation has been studied for the SIT in a nonlinear medium without the PBG structure [27]. Substituting Eq. (3.10) and $a_\pm(z,t)=\pm a(\tau)/\sqrt{2}$ into Eq. (3.2b), and then substituting Eq. (3.9) and $\partial\varphi/\partial\tau=2c_0/a(\tau)^2$ into Eq. (3.7), we find that both of the resulting equations lead to

$$\frac{\partial^2 a}{\partial\tau^2}=\frac{4c_0^2}{a^3}+\gamma_1 a+\gamma_3 a^3, \tag{3.11}$$

where

$$\gamma_1\equiv\frac{1}{c_2}-\frac{c_1^2}{4c_2^2}=\frac{1}{|\beta_2^e|L_D}, \quad \gamma_3\equiv\frac{3\mu^2}{4\hbar^2}=\frac{2\Gamma_\nu}{|\beta_2^e|}. \tag{3.12}$$

For $c_0\neq 0$, Eq. (3.11) has a distortionless pulse-train solution given by the Jacobi elliptic function. Such pulse-train propagation results from the energy of resonant atoms periodically oscillating between the ground state and the upper state. For a resonance medium without PBG structure, a real shape-preserving pulse train has been observed in the experiment [30]. Here we focus our attention on a single-pulse solution to Eq. (3.11). For $c_0=0$, we obtain $a(\tau)=A_0\,\mathrm{sech}(\tau/T_0)$, where $A_0=\sqrt{|\beta_2^e|/(\Gamma_\nu T_0^2)}=2\sqrt{2}\hbar/(\sqrt{3}\mu T_0)$ is the pulse amplitude and $T_0=1/\sqrt{\gamma_1}$ is the pulse width. Consequently, we obtain

$$E_\pm(\xi,\tau)=\pm\frac{A_0}{\sqrt{2}}\mathrm{sech}\left(\frac{\tau}{T_0}\right)e^{i[(\xi/2L_D)+Qz-(-\Delta\omega_B+\Omega_+)t]}, \tag{3.13}$$

where the dispersion length is $L_D=T_0^2/|\beta_2^e|$. Because the central frequency $\omega_0=\omega_B-\Delta\omega_B+\Omega_+$ of this optical field is inherently located at the effective band gap edge, Eq. (3.13) represent a Bragg soliton. This soliton undergoes the effective third-order nonlinearity and quadratic grating dispersion expressed in Eq. (3.8). Furthermore, such a soliton solution also satisfies the atomic Bloch equations. Hence it indicates the coexistence of a SIT soliton and a Bragg soliton. This mixed state is referred to as a SIT-Bragg soliton. Note that the characteristics of the effective PBG structure described by Eq. (3.4) is not fixed by the associated medium parameters. Such an effective model can be determined by the input pulse width T_0 incorporated with either the atomic frequency detuning $\Delta\omega_{r0}$ or the Bragg frequency detuning $\Delta\omega_0$. Therefore, a SIT-Bragg soliton can exist deep inside the original forbidden gap as long as $\Delta\omega_0=-c_1/(2c_2)<\kappa/\beta_1$.

IV. CHARACTERISTICS OF SIT-BRAGG SOLITON

To examine the existence of a SIT-Bragg soliton, we study the soliton solution in an As_2S_3-based fiber Bragg grating (As_2S_3-FBG) doped uniformly with Lorentzian line-shape two-level atoms. The As_2S_3-based fiber is a type of chalcogenide-glass fiber with the Kerr nonlinearity being two orders of magnitude higher than the value of silica-glass fiber [32,33]. The fabrication of an As_2S_3-FBG has also been reported [34]. The material parameters for such an As_2S_3-FBG are assumed to be $n_0=n(\omega_0)=2.39$, $\beta_0=5.9\times10^6\ \mathrm{m}^{-1}$, $\beta_1=7.9\times10^{-9}$ s/m, and $n_2=2.5\times10^{-20}\ \mathrm{m}^2/\mathrm{V}^2$ at 1550 nm wavelength region. The coupling coefficient of the Bragg grating is $\kappa=100\ \mathrm{cm}^{-1}$, corresponding to the index vibration $\delta n_g=0.005$ at the Bragg wavelength $\lambda_B=1553$ nm. For the embedded resonant atoms, the Lorentzian line-shape function is written as

$$g(\Delta\omega-\Delta\omega_{r0})=(\Delta\omega_a/2\pi)/[(\Delta\omega-\Delta\omega_{r0})^2+(\Delta\omega_a/2)^2],$$

where $\Delta\omega_a=2\pi\Delta f_a$ is the full width at half maximum (FWHM) of $g(\Delta\omega-\Delta\omega_{r0})$. We assume that $\Delta f_a=1472$ GHz, $\mu=1.4\times10^{-32}$ C m, and $N_D=8.0\times10^{26}\ \mathrm{m}^{-3}$. Note that the large Δf_a is realistic for erbium atoms. In addition, to numerically solve the parameters of a SIT-Bragg soliton, we have to assume $\Delta\omega_a\gg 1/T_0$, which indicates that the spectral width of the pulse is much less than the spectral width of the inhomogeneous-broadening linewidth. Hence the soliton pulse width in our numerical study must satisfy $T_0\gg 0.1$ ps.

The soliton pulse width and group velocity now can be numerically obtained according to the characteristic equations for the SIT-Bragg soliton, which are rewritten as

$$\Delta\omega_0=-\Delta\omega_B+\Omega_+=-c_1/(2c_2), \tag{4.1a}$$

$$A_0=\sqrt{|\beta_2^e|/(\Gamma_\nu T_0^2)}=2\sqrt{2}\hbar/(\sqrt{3}\mu T_0), \tag{4.1b}$$

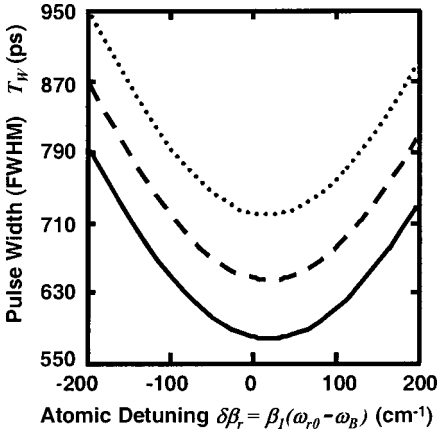

FIG. 2. Pulse width of the SIT-Bragg solitons as a function of atomic detuning $\delta\beta_r$ at carrier detuning $\delta\beta_0 = 20\ \mathrm{cm}^{-1}$ (dotted line), $\delta\beta_0 = 22\ \mathrm{cm}^{-1}$ (dashed line), and $\delta\beta_0 = 24\ \mathrm{cm}^{-1}$ (solid line). Note that the original band gap edge of the As_2S_3-based fiber grating is located at $\pm\kappa = \pm 100\ \mathrm{cm}^{-1}$. The FWHM curve for a fixed $\delta\beta_0$ is symmetric to $\delta\beta_r = \delta\beta_0$. Thus the minimum pulse width (maximum peak intensity) required for a SIT-Bragg soliton occurs on exact atomic resonance $\omega_0 = \omega_{r0}$.

where $\Delta\omega_B = -\delta\beta_e/\beta_1^e$ and $\Omega_+ = \kappa\gamma/\beta_1^e$; likewise $\gamma = 1/\sqrt{1-\nu^2}$ is approximated by $1+\nu^2/2$ under the slow-velocity limitation. Because these characteristic equations strictly constrain the coexistence of a SIT and a Bragg soliton, the soliton pulse width and group velocity are uniquely determined for the Bragg detuning, atomic detuning, and given material parameters. Figure 2 first shows the pulse width (FWHM, $T_W \approx 1.763T_0$) of the SIT-Bragg solitons as a function of atomic detuning $\delta\beta_r$, when the carrier detuning is located at $\delta\beta_0 = 20\ \mathrm{cm}^{-1}$ (dotted line), $\delta\beta_0 = 22\ \mathrm{cm}^{-1}$ (dashed line), and $\delta\beta_0 = 24\ \mathrm{cm}^{-1}$ (solid line). The FWHM curve for a fixed $\delta\beta_0$ is symmetric to $\delta\beta_0 = \delta\beta_r$; thus the minimum pulse width required for a SIT-Bragg soliton occurs on exact atomic resonance $\omega_0 = \omega_{r0}$. The influence of Bragg detuning on the required pulse width is further shown in Fig. 3. For the atomic on-resonance case ($\delta\beta_r = 0$), Fig. 3(a) shows that a larger Bragg detuning implies a narrower pulse width for the existence of a SIT-Bragg soliton. For $\delta\beta_0 < 40\ \mathrm{cm}^{-1}$, the required pulse width rapidly increases. Figure 3(b) shows the corresponding peak intensity required for a SIT-Bragg soliton at $\delta\beta_r = 0$ as a function of $\delta\beta_0$. The peak intensity of a SIT-Bragg soliton is defined by $I_P = (n_0/2)(\sqrt{\varepsilon_0/\mu_0})A_0^2$, where ε_0 is the vacuum permittivity [13,14]. Obviously, for $\delta\beta_0 > 40\ \mathrm{cm}^{-1}$, the intensity curve shows the approximately linear dependence of the peak intensity and the Bragg detuning of a SIT-Bragg soliton. Notice that Fig. 3 does not exhibit the pulse width and peak intensity for $0 < \delta\beta_0 < 20$ because the required pulse width for this range dramatically exceeds 1 ns that is not much less than the atomic relaxation times. The inset of Fig. 3(a) presents the remarkably increasing trend of the pulse width for a small carrier detuning. From an experimental viewpoint, the atomic relaxation processes would incoherently absorb the pulse energy for $0 < \delta\beta_0 < 20$.

Figure 4(a) shows the effective linear dispersion curves

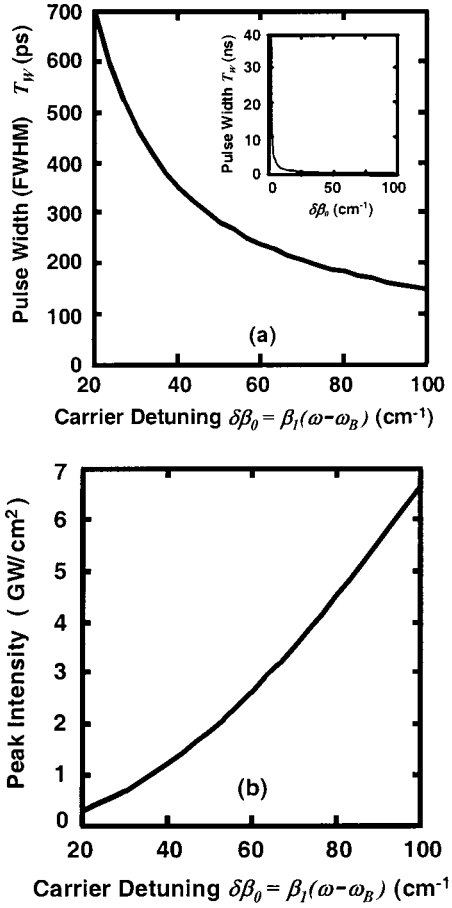

FIG. 3. (a) Pulse width and (b) corresponding peak intensity required for the SIT-Bragg solitons as a function of carrier detuning $\delta\beta_0$ on exact atomic resonance $\delta\beta_r = 0$. The inset shows that the pulse width rapidly increases as the carrier detuning decreases.

and Fig. 4(b) shows the nonlinear dispersion curves [31] of the effective PBG structure for a SIT-Bragg soliton with carrier detuning $\delta\beta_0 = 100\ \mathrm{cm}^{-1}$, atomic detuning $\delta\beta_r = 0\ \mathrm{cm}^{-1}$, and peak intensity $I_P = 6.70\ \mathrm{GW/cm}^2$. The dashed curves show the original linear case. Because this soliton is located at the original upper band gap edge ($\delta\beta_0 = \kappa = 100\ \mathrm{cm}^{-1}$), the position of the effective upper band gap edge remains unchanged at the original PBG edge. However, the width of the effective band gap has been narrowed from $2\kappa = 200\ \mathrm{cm}^{-1}$ to $133.33\ \mathrm{cm}^{-1}$. When the effective nonlinearity is taken into account, the effective upper band gap edge has been down shifted to $45.58\ \mathrm{cm}^{-1}$ due to the intense peak intensity. By contrast, Fig. 4(c) also shows the effective linear dispersion curves, and Fig. 4(d) shows the nonlinear dispersion curves of the effective PBG structure for a SIT-Bragg soliton with $\delta\beta_0 = 20\ \mathrm{cm}^{-1}$, $\delta\beta_r = 0\ \mathrm{cm}^{-1}$, and $I_P = 0.30\ \mathrm{GW/cm}^2$. The effective linear dispersion relation shows that the effective upper band gap edge has been shifted to $20\ \mathrm{cm}^{-1}$ and the width of the effective forbidden band has become $57.12\ \mathrm{cm}^{-1}$. Because the peak intensity in this case is much smaller than that in Fig. 4(b), the effective upper band gap edge is down shifted only $6.51\ \mathrm{cm}^{-1}$ from the upper band gap edge of its linear dispersion relation.

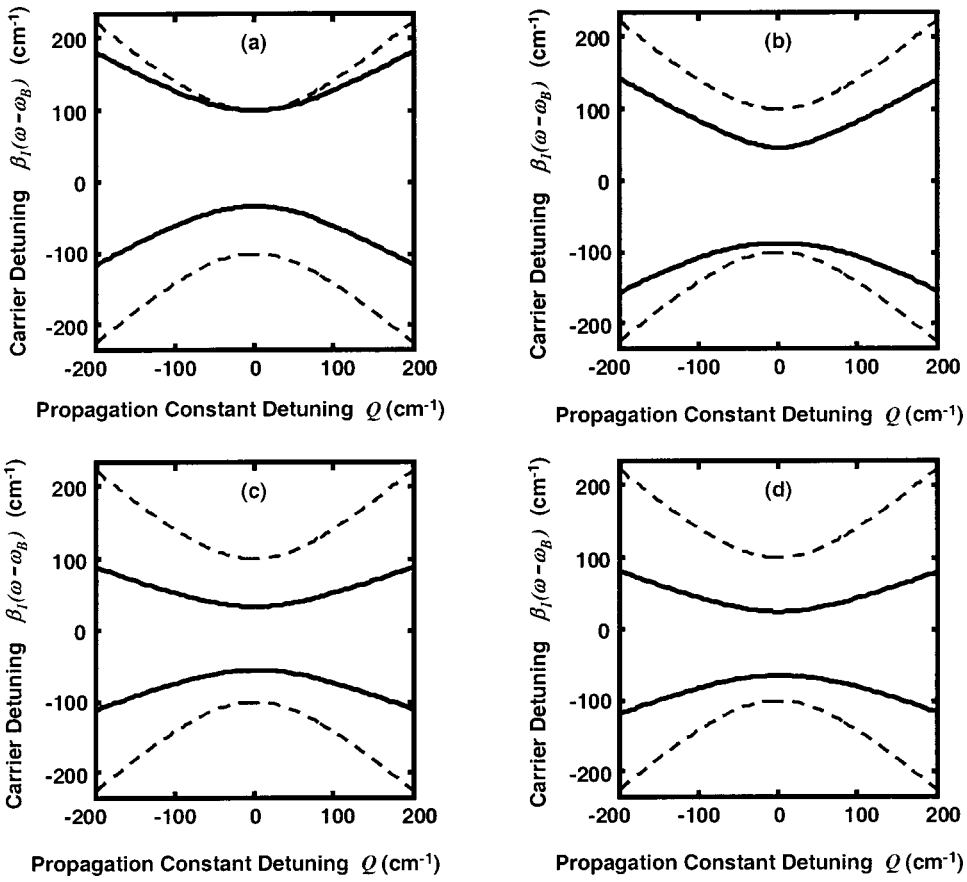

FIG. 4. (a) Effective linear dispersion curves and (b) nonlinear dispersion curves of the effective PBG structure for a SIT-Bragg soliton with carrier detuning $\delta\beta_0 = 100\ \mathrm{cm}^{-1}$ and peak intensity $I_P = 6.70\ \mathrm{GW/cm}^2$. For comparison, we also show (c) effective linear dispersion curves and (d) nonlinear dispersion curves for another SIT-Bragg soliton with $\delta\beta_0 = 20\ \mathrm{cm}^{-1}$ and peak intensity $I_p = 0.30\ \mathrm{GW/cm}^2$. Dashed curves show the original linear case without resonant dopants.

Consequently, a SIT-Bragg soliton is an optical pulse satisfying the Bragg soliton propagation in an effective undoped PBG structure.

The group velocity of such a SIT-Bragg soliton in the range of $20 < \delta\beta_0 < 100$ is shown in Fig. 5(a). The quantity of ν_g approximately corresponds to 1/250 of the speed of light in vacuum. This propagating delay originates from both the SIT effect and the multiple scattering due to the periodic structure. Furthermore, the relativistic velocity $\nu = \beta_1^e \nu_g$ is shown in Fig. 5(b). The magnitude of ν is less than 0.05. Thus the slow-velocity limit is valid for the SIT-Bragg soliton. It is well known that one of the attractive characteristics of a Bragg soliton is the reduction of its group velocity. The experiments have shown that a Bragg soliton with 80-ps width can travel with the velocity as low as 50% of the light speed in an unprocessed fiber [14]. Hence all optical buffer based on the slow propagation of a Bragg soliton is an ongoing challenge. Figure 6(a) shows the velocity of a SIT-Bragg soliton as a function of the coupling coefficient at $\delta\beta_0 = 60\ \mathrm{cm}^{-1}$ and $\delta\beta_r = 0\ \mathrm{cm}^{-1}$. When the coupling coefficient is increased, the group velocity of a SIT-Bragg soliton is smoothly decreased. It is obvious that a larger index variation of the periodic structure leads to the more serious Bragg scattering. The magnitude of the soliton velocity maintains its order at 10^6 m/s due to the SIT effect. The relativistic velocity $\nu = \beta_1^e \nu_g$ is shown in the inset of Fig. 6(a). The slow-velocity limitation for our doped As_2S_3-based FBG with coupling coefficient from $\kappa = 20\ \mathrm{cm}^{-1}$ to $\kappa = 100\ \mathrm{cm}^{-1}$ is also valid. Figure 6(b) shows the corresponding pulsed width required for the SIT-Bragg soliton. The relation between the pulse width and the PBG coupling coefficient is approximately a linear dependence. We emphasize that the slow-velocity limit is invalid for a SIT-Bragg soliton in an erbium-doped silica-based FBG. Consequently, in this paper we focus our numerical study on a doped As_2S_3-based FBG to make the slow-velocity limit valid and reduce the required peak intensity. Alternatively, an integrated AlGaAs waveguide grating doped with resonant atoms could be a suitable PBG medium for the observation of a SIT-Bragg soliton, because the AlGaAs waveguides have sufficient power-handling capabilities to reduce the required peak intensity [10]. A large coupling coefficient of the AlGaAs waveguide grating also can be easily achieved for the slow-velocity limitation of a SIT-Bragg soliton.

Finally, we stress that although our results for a SIT-Bragg soliton in a doped As_2S_3-based FBG are realistic, the doping concentration adopted in the numerical study is two orders of magnitude larger than the value of a typically erbium-doped fiber. Figure 7 shows the soliton pulse width as a function of the doping concentration at $\delta\beta_0 = 60\ \mathrm{cm}^{-1}$ and $\delta\beta_r = 0\ \mathrm{cm}^{-1}$. It presents the remarkably increasing trend of the pulse width for a small doping concentration. From an experimental viewpoint, the atomic relaxation processes would incoherently absorb the pulse energy for low concentration. Nevertheless, it will be interesting to study the suitable material, for example, an erbium-doped AlGaAs waveguide grating with high doping density, to experimentally investigate the existence of a SIT-Bragg soliton.

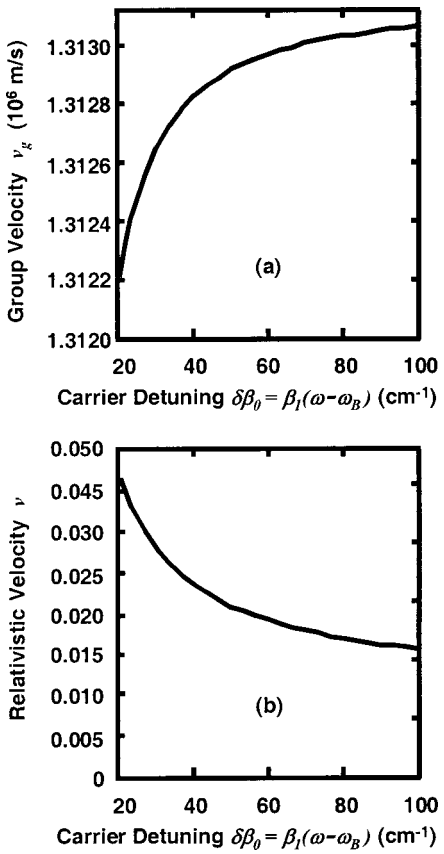

FIG. 5. (a) Group velocity and (b) relativistic velocity $\nu = \beta_1^e v_g$ of the SIT-Bragg solitons as a function of carrier detuning $\delta\beta_0$ on exact atomic resonance $\delta\beta_r = 0$. Notice that the trends of the group velocity curve and the relativistic velocity curve are opposite, because the effective group velocity $1/\beta_1^e$ describing the velocity of each optical frequency component (CW case) also varies with the Bragg detuning. The relativistic velocity shows that the slow-velocity limit is valid for a SIT-Bragg soliton in a doped As_2S_3-based PBG structure.

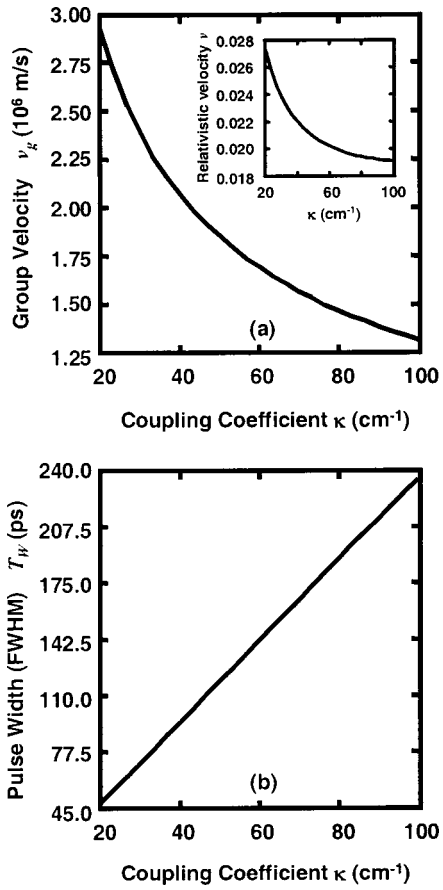

FIG. 6. (a) Group velocity and (b) pulse width of the SIT-Bragg solitons as functions of the coupling coefficient of a doped As_2S_3-based PBG structure.

V. DISCUSSION AND CONCLUSIONS

In this paper, we adopt a uniformly doped nonlinear PBG model to study the SIT effect deep inside the forbidden band. The fundamental work of SIT in such a uniformly doped PBG structure has been studied in Ref. [22]. In this previous study, the authors reduce the NLCMEs with polarization envelopes by directly expanding the dispersion relation of the pure grating. Hence their model represented by our notations can be written as

$$i\frac{\partial E}{\partial \tau} - \frac{1}{2}\beta_2^G \frac{\partial^2 E}{\partial \xi^2} + \Gamma |E|^2 E + \frac{\mu_0 \omega_B^2}{2\beta_0} P = 0, \qquad (5.1)$$

where β_2^G is quadratic dispersion for pure grating. Figure 8(a) shows the pure grating dispersion [14,31] of an As_2S_3-based FBG as a function of carrier detuning. The inset shows that when the carrier is near the original band gap edge ($\kappa = 100\ \mathrm{cm}^{-1}$), the pure grating dispersion trends to infinity. Therefore, a SIT-gap soliton is a distortionless optical pulse resulting from this pure grating dispersion, balancing with both the material Kerr nonlinearity and the resonant effects determined by the Bloch equations. Because of this balance based on the pure grating dispersion, the doping concentration and the atomic detuning frequency can dramatically change the characteristics of a SIT gap soliton when the carrier detuning is close to the original band gap edge. By contrast, in our study, the NLCMEs with polarization envelopes are first reduced to effective NLCMEs, and these effective NLCMEs are subsequently reduced to effective NLS equation. On the basis of such reduction, our effective model completely involves the dispersion due to the polarization. In particular, our model simplifies the resonant effects to effective dispersion and effective nonlinearity, even if the atomic line shape is inhomogeneously broadening. Figure 8(b) shows our effective grating dispersion of an As_2S_3-based FBG uniformly doped with resonant atoms as a function of carrier detuning. Because the resonant effects have been taken into account and a SIT-Bragg soliton is inherently located at the effective band gap edge, such an effective quadratic dispersion is much larger than the pure grating dispersion for a fixed carrier detuning. Furthermore, the slow propagation caused by the SIT effect can lead to the SIT-induced dispersion [23,29]. This induced dispersion should be considered by keeping the second derivative of the electromagnetic field with respect to the propagation distance. The SIT-induced dispersion can be written as

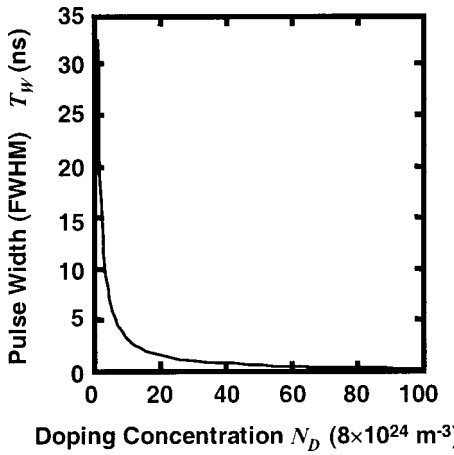

FIG. 7. Pulse width of a SIT-Bragg solitons as a function of the doping concentration of the erbium atoms at $\delta\beta_0=60\ \mathrm{cm}^{-1}$ and $\delta\beta_r=0\ \mathrm{cm}^{-1}$. Because the pulse width should be much less than the atomic relaxation times, the doping concentration adopted in the numerical study is two orders of magnitude larger than the value of typically erbium-doped fiber.

$$\beta_2^{\mathrm{SIT}}=-(\Delta\beta_1^2+2\beta_1\Delta\beta_1)/\beta_0, \tag{5.2}$$

where $\Delta\beta_1=1/\nu_g-\beta_1$. Figure 8(c) shows the SIT-induced dispersion based on the group velocity shown in Fig. 5(a). Obviously, the SIT-induced dispersion is much smaller than the effective quadratic dispersion originating from the effective periodic structure. Hence this induced dispersion due to the slow propagation is negligible for a SIT-Bragg soliton.

According to Sec. IV and the above-mentioned discussion, the physical interpretation for a SIT-Bragg soliton can be described as follows: A uniformly doped PBG structure can be regarded as an effective undoped PBG structure. The resonant atoms lead to the effective grating dispersion and resonant enhanced nonlinearity. Hence the original forbidden band has been shifted. Furthermore, an instantaneous nonlinearity response due to the intense pulse also shifts the stop band. As a result, a nonlinear optical pulse that satisfies the soliton pulse shape and obeys the SIT chirping relation renders the PBG ''transparent.'' In particular, for distortionless propagation in the uniformly doped nonlinear PBG structure, the effective quadratic dispersion has to balance with the effective third-order nonlinearity. Although our results exhibit such a SIT soliton, we emphasize that the population difference $w=w_0+2w_1\cos[2\psi(z,t)+2\beta_g z]$ is a basic assumption. We use this assumption to get a closed set of atomic Bloch equations. Strictly speaking, we have neglected all higher-order spatial harmonics of the population difference. Hence the theoretical model and its analytic solutions in our work are constrained by this assumption. On the other hand, such an assumption can be avoided by assuming that the resonant atoms are periodically doped in a host medium [16–21]. However, from a practical viewpoint, the fabrication of a uniformly doped PBG model is simple. It would be interesting to study the impacts of the higher-order spatial harmonics on the stability of the solitary propagation. Consequently, the experimental observation of a SIT-Bragg soliton in a doped nonlinear PBG medium would be an attractive subject, which can lead to the practical expansions of Bragg grating solitons in the vast area of light wave systems.

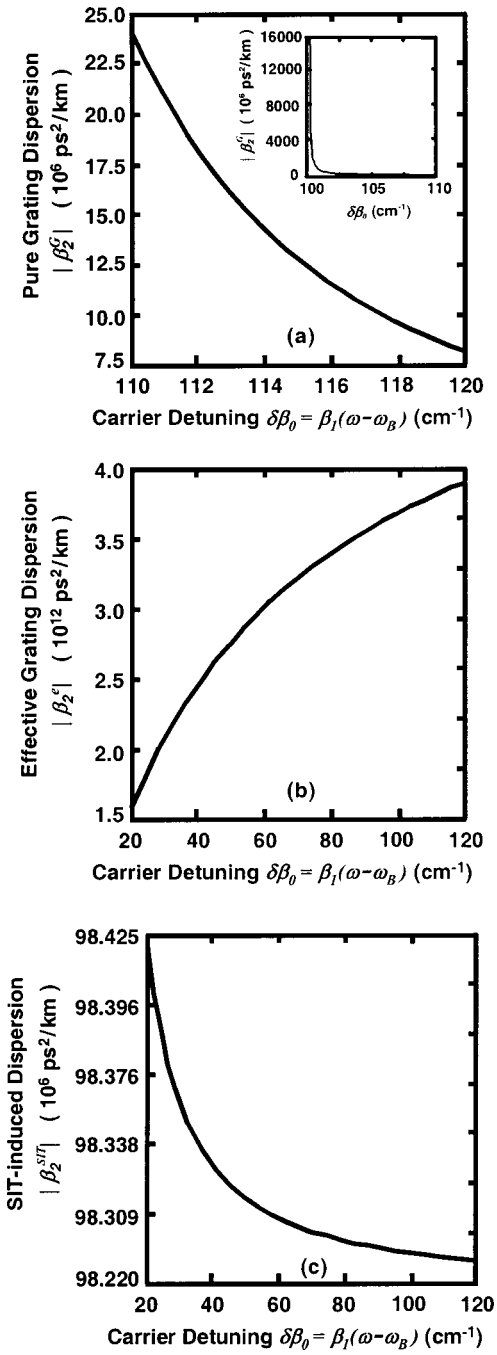

FIG. 8. (a) Pure grating dispersion adopted in Ref. [22] for balancing with the material Kerr nonlinearity and resonant effects. The inset shows that when the carrier is near the original band gap edge ($\kappa=100\ \mathrm{cm}^{-1}$), the pure grating dispersion trends to infinity. (b) Effective grating dispersion adopted in our study for balancing with the effective nonlinearity. (c) SIT-induced dispersion resulting from the slow propagation.

In summary, we have found an approximate soliton solution to the Bloch-NLCMEs, and studied the characteristics of such solitons in an As_2S_3-based PBG structure doped uniformly with Lorentzian line-shape two-level atoms. Our re-

sults indicate the existence of a SIT-Bragg soliton even within the forbidden band of the PBG structure. Such coexistence originates from the offset of the stop band due to the effective quadratic dispersion and the resonant enhanced nonlinearity. The intense optical pulse also shifts the band gap by nonlinear response and therefore propagates through the original forbidden band. Consequently, the SIT renders the periodic structure ''transparent,'' and facilitates the effective Bragg-soliton propagation in this uniformly doped nonlinear PBG structure.

ACKNOWLEDGMENT

This work was supported by the Academic Excellence program of R.O.C. Ministry of Education under Contract No. 90-E-FA06-1-4-90X023.

[1] E. Yablonovitch, Phys. Rev. Lett. **58**, 2059 (1987).
[2] S. John, Phys. Rev. Lett. **58**, 2486 (1987); Phys. Today **44**(5), 32 (1991).
[3] A. B. Aceves and S. Wabnitz, Phys. Lett. A **141**, 37 (1989).
[4] A. B. Aceves, Chaos **10**, 584 (2000).
[5] C. M. de Sterke and J. E. Sipe, in *Progress in Optics*, edited by E. Wolf (North-Holland, Amsterdam, 1994), Vol. 33, Chap. 3.
[6] J. Feng and F. K. Kneubühl, IEEE J. Quantum Electron. **29**, 590 (1993).
[7] S. John and N. Aközbek, Phys. Rev. Lett. **71**, 1168 (1993).
[8] N. Aközbek and S. John, Phys. Rev. E **57**, 2287 (1998).
[9] U. Mohideen, R. E. Slusher, V. Mizrahi, T. Erdogan, M. Kuwata-Gonokami, P. J. Lemaire, J. E. Sipe, C. M. de Sterke, and N. G. R. Broderick, Opt. Lett. **20**, 1674 (1995).
[10] P. Millar, R. M. De La Rue, T. F. Krauss, J. S. Aitchison, N. G. R. Broderick, and D. J. Richardson, Opt. Lett. **24**, 685 (1999).
[11] J. E. Sipe and H. G. Winful, Opt. Lett. **13**, 132 (1988).
[12] B. J. Eggleton, R. E. Slusher, C. M. de Sterke, P. A. Krug, and J. E. Sipe, Phys. Rev. Lett. **76**, 1627 (1996).
[13] B. J. Eggleton, C. M. de Sterke, and R. E. Slusher, J. Opt. Soc. Am. B **14**, 2980 (1997).
[14] B. J. Eggleton, C. M. de Sterke, and R. E. Slusher, J. Opt. Soc. Am. B **16**, 587 (1999).
[15] C. M. de Sterke and B. J. Eggleton, Phys. Rev. E **59**, 1267 (1999).
[16] B. I. Mantsyzov, Phys. Rev. A **51**, 4939 (1995).
[17] B. I. Mantsyzov, Opt. Commun. **189**, 275 (2001).
[18] B. I. Mantsyzov and R. A. Sil'nikov, Pis'ma Zh. Eksp. Teor. Fiz. **74**, 511 (2001) [JETP Lett. **74**, 456 (2001)].
[19] A. E. Kozhekin and G. Kurizki, Phys. Rev. Lett. **74**, 5020 (1995).
[20] A. E. Kozhekin, G. Kurizki, and B. A. Malomed, Phys. Rev. Lett. **81**, 3647 (1998).
[21] M. Blaauboer, G. Kurizki, and B. A. Malomed, Phys. Rev. E **62**, R57 (2000).
[22] N. Aközbek and S. John, Phys. Rev. E **58**, 3876 (1998).
[23] H. Y. Tseng and S. Chi, IEEE J. Sel. Top. Quantum Electron. **8**, 681 (2002).
[24] S. L. McCall and E. L. Hahn, Phys. Rev. Lett. **18**, 908 (1967).
[25] J. H. Eberly, Phys. Rev. Lett. **22**, 760 (1969).
[26] M. D. Crisp, Phys. Rev. Lett. **22**, 820 (1969).
[27] L. Matulic and J. H. Eberly, Phys. Rev. A **6**, 822 (1972).
[28] M. Nakazawa, Y. Kimura, K. Kurokawa, and K. Suzuki, Phys. Rev. A **45**, 23 (1992).
[29] S. Chi, T. Y. Wang, and S. Wen, Phys. Rev. A **47**, 3371 (1993).
[30] J. L. Shultz and G. J. Salamo, Phys. Rev. Lett. **78**, 855 (1997).
[31] G. P. Agrawal, *Applications of Nonlinear Fiber Optics* (Academic, San Diego, 2001).
[32] M. Asobe, T. Kanamori, and K. Kubodera, IEEE Photonics Technol. Lett. **4**, 362 (1992).
[33] M. Asobe, T. Kanamori, and K. Kubodera, IEEE J. Quantum Electron. **29**, 2325 (1993).
[34] M. Asobe, T. Ohara, I. Yokohama, and T. Kaino, Electron. Lett. **32**, 1611 (1996).